Soft Matter

PAPER

View Article Online
View Journal | View Issue

Stability of polymer glasses vitrified under stress

Cite this: *Soft Matter*, 2014, **10**, 1572

Laura A. G. Gray and Connie B. Roth*

How stress or strain imparts mobility to glasses is a scientific issue linking ideas of jamming and the glass transition across colloids, granular materials, polymers, and molecular glasses. Here, we address for the first time how stress applied during vitrification, formation of the glassy state by a temperature quench, affects the subsequent stability of the glassy state, even after the stress has been removed. Using entangled polymers that are easily manipulated mechanically above the glass transition temperature, we find that the resulting polymer glasses become less stable, exhibiting a higher physical aging rate, when stress is applied while rapidly cooling the polymer films. The data show an initial plateau value at low stress, before transitioning rapidly to a higher aging rate at larger stress. These results are suggestive of the glassy system being left trapped in a less stable, higher energy state with faster physical aging rate when stressed above some minimum value during vitrification.

Received 6th August 2013
Accepted 8th January 2014

DOI: 10.1039/c3sm52113c

www.rsc.org/softmatter

Glasses are a non-equilibrium state of matter formed when packing frustration leaves the system trapped in a configuration that does not correspond to the global energy minimum of the equilibrium glass or crystal. Trapped in this higher energy state with excess free volume, glasses evolve in time leading to densification of the material and a host of other property changes, a process termed physical aging. A scientific description of these dynamics is extremely challenging because of the many-body interactions involved and our lack of a statistical mechanics description of non-equilibrium phenomena. In recent years, numerous studies have observed anomalous glassy physical aging dynamics as the sample size is reduced,[1] some occurring at length scales much larger than where boundary effects are known to alter the glass transition.[2,3] It has been suggested that unintended stresses imparted to the material during glass formation might be the underlying cause of the observed faster physical aging.[4,5] Here we directly test this assertion and demonstrate that stress present during the thermal quench is an important parameter affecting the subsequent physical aging.

Glassy behavior is common to a variety of different systems that all exhibit frustration upon cooling or densification, leading to the kinetic arrest of the system. Molecular glass formers, as common as silica (window glass) and amorphous polymers (transparent plastics), form a glass upon cooling when the available thermal energy is no longer able to equilibrate molecular configurations at the glass transition temperature (T_g). Colloidal systems (milk) and granular materials (sand) become jammed into a glassy state at high volume fractions, while spin glasses occur when the magnetization becomes frustrated. The glass transition defies theoretical description because of its pseudo nature, depending on the rate at which the glassy state is formed and there being little structural difference between the liquid and glassy state. Significant progress has been made in our understanding of the glass transition by comparing similarities across different systems. One such unifying concept is the jamming phase diagram,[6,7] which proposes a possible equivalence between temperature, density, and stress as different control parameters for the onset of rigidity associated with glass formation. Although the specific shape of the jamming diagram and the extent to which jamming (a zero-temperature phenomenon) and the glass transition can be related are under debate,[7–10] for the present discussion we are intrigued simply by the possible interplay between temperature and stress as we investigate glass formation by temperature quench at non-zero stress. A related issue of current debate is the extent to which mechanical deformation (stress) can be used to increase mobility and possibly "rejuvenate" a glass, equivalent to re-equilibrating the glass above its T_g.[11–13]

Recent studies have shown that molecular mobility of glasses does not correlate with free volume,[14,15] but instead depends on the material's position within a potential energy landscape.[16,17] The potential energy landscape (PEL) picture is an important conceptual framework for understanding the glass transition and dynamics in frustrated systems, providing a topographical view of the energy states of the system that depend on the configurational coordinates of the structural units.[18,19] The rugged multidimensional landscape describing amorphous materials has many local energy minima within which the system can become easily trapped, preventing it from finding the more energetically favorable global minimum. The various energy minima are arranged into "metabasins" within

Department of Physics, Emory University, Atlanta, GA 30322, USA. E-mail: cbroth@emory.edu

which local β-relaxations associated with physical aging drive the system towards a common local minimum or "basin of attraction".[20] At higher temperatures above T_g, the system is free to transition between metabasins *via* α-relaxations. The classic cooling rate dependence of glass formation where faster cooling rates lead to less stable glasses with faster physical aging rates is understood as the system being trapped in shallower, higher energy metabasins.[18,21] In contrast, a slower cooling rate allows the system more time to explore the rugged PEL enabling it to reach a deeper, lower energy metabasin with a correspondingly slower physical aging rate.

Within the PEL framework, stress induced molecular mobility has been centered around the idea originally put forward by Eyring[22] of a stress activated barrier hopping or landscape tilting mechanism.[17,23–27] A stress or strain imparted to the glass acts to deform or tilt the PEL, such that sufficiently large values can drive the system up the PEL[23] appearing to effectively reverse physical aging or "rejuvenate" the glass.[11,13] However, mechanical deformation can also transform the glass to a different energy state.[13,17,23] Studies of how mechanical deformation imparts mobility that alters glassy dynamics have almost exclusively been conducted on systems where the glass was formed stress free.[11–13,23,24,28–31] Here, we investigate how stress applied during vitrification of the glass can increase its physical aging rate appearing to leave the system trapped in a less stable, higher energy state.

Molecular mobility of glassy polymer films can be characterized by measuring the physical aging rate. The speed at which the glassy material undergoes densification on a logarithmic timescale, often termed structural relaxation, depends on the nature of the local energy states within which the system is trapped providing a measure of the local slope of the metabasin.[18,20] The volumetric aging rate, characterizing the rate of densification in the material, has been historically defined as $\beta = -\partial(V/V_\infty)/\partial(\log t)$, where V_∞ represents the equilibrium volume of the glass at the aging temperature.[32,33] Because it is often not possible to reach equilibrium at aging temperatures far below T_g,[34,35] the volume at equilibrium is typically approximated by a linear extrapolation of the liquid line.[35,36] For a polymer film whose area is constrained to be fixed during the aging process, volume contraction occurs only in the direction perpendicular to the substrate such that the physical aging rate can be evaluated from the decrease in film thickness h as $\beta = -\partial(h/h_0)/\partial(\log t)$.[2,4,5,36] We take h_0 to be the absolute film thickness at an aging time of 10 min, which has been previously demonstrated to give values of β equivalent to using h_∞, the extrapolated value of the film thickness at equilibrium.[36] Ellipsometry is used to measure the decrease in film thickness h and increase in index of refraction $n(\lambda)$ of the polymer films associated with densification of the material during structural relaxation. The resulting data are plotted typically as normalized film thickness (h/h_0) *versus* the logarithm of the aging time, as depicted in Fig. 1, such that the aging rate is effectively given by the slope. Specific details of the ellipsometry measurements and analysis have been given previously.[2,4,5,36] For this particular study, we have used polystyrene (PS) of three different molecular weights (M_w = 1440 kg mol^{-1}, M_w/M_n = 1.04; M_w = 650 kg mol^{-1}, M_w/M_n = 1.06; M_w = 289 kg mol^{-1}, M_w/M_n = 2.19). Films from 150 to 1700 nm in thickness were formed by spin-coating PS from toluene onto freshly cleaved mica, and subsequently annealing under vacuum for at least 12 h at 120 °C (T_g + 20 °C) to remove residual solvent and relax chain conformations. Films cut to a width of 13 mm were floated off mica onto the surface of deionized water and captured onto a specially designed aluminum frame, where the initial length of the free-standing film was 9.15 mm. The aluminum frame is designed to be mounted vertically into a home-built jig that encloses the film in a heater while allowing us to apply a known uniaxial tension to the film *via* a cantilever arm with a variable counterweight. The sliding frame can be pinned in place allowing us to control when and for how long stress is applied to the film. The stress applied to the film was varied by changing both the counterweight and the film thickness. Strain was measured by comparing the length of the film digitalized from images captured before and after stress was applied.

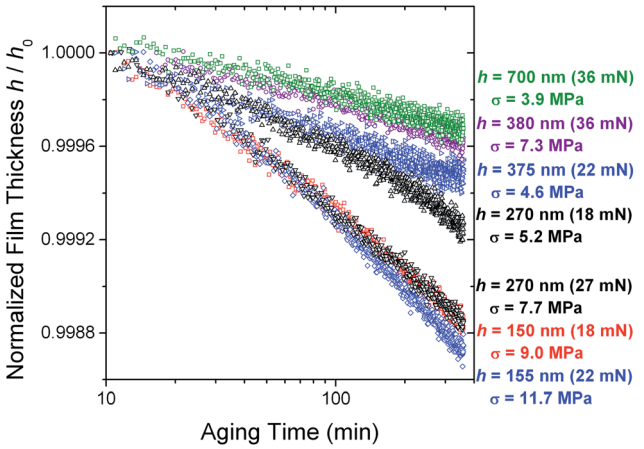

Fig. 1 Decrease in film thickness with aging time due to densification of the glass during structural relaxation. Physical aging rate β determined from the slope of a plot of normalized film thickness h/h_0 *versus* logarithm of aging time. The physical aging behavior was found to correlate with the stress σ experienced by the films during vitrification, which was altered by changing both the film thickness h and tension applied. For example, a 270 nm thick film (black data) has an aging rate of $(4.44 \pm 0.65) \times 10^{-4}$ when a stress of 5.2 MPa is applied, compared to an aging rate of $(7.14 \pm 0.65) \times 10^{-4}$ with a stress of 7.7 MPa. Similarly, for a tension of 22 mN (blue data), the aging rate was found to be $(3.50 \pm 0.65) \times 10^{-4}$ for a 375 nm thick film compared to $(8.43 \pm 0.65) \times 10^{-4}$ for a 155 nm thick film. Data shown are for 1440 kg mol^{-1} M_w polystyrene (PS) films.

Physical aging measurements were initiated by equilibrating the films within the jig for 30 min at T_g + 20 °C without any stress applied. Then a constant stress between 1.0 and 15.0 MPa was applied to the film for 2 min by releasing the pins holding the cantilever arm. After two minutes, the heater was turned off and the enclosure opened. The films were allowed to cool for 2 min before being removed from the jig and gently transferred onto silicon wafers for the aging measurements. In previous work we have calculated that such a protocol cools the films rapidly through T_g with a quench rate in excess of 7000 K min^{-1}.[4] Transferring the films onto silicon allows us to reliably measure the aging rate, as has been previously demonstrated.[4]

The ellipsometer hot-stage was pre-equilibrated to the aging temperature of 65 °C, corresponding to the peak in aging rate for PS,[2,36] such that the samples quickly reached the aging temperature once transferred to the ellipsometer.

Fig. 1 plots the decrease in normalized film thickness h/h_0 as a function of aging time that results from densification of the films during structural relaxation. Data shown are for 1440 kg mol^{-1} M_w PS films of thicknesses between 150 and 700 nm with different amounts of tension applied shortly before and during the thermal quench. The applied stress σ during glass formation was found to strongly affect the resulting physical aging rate of the films. Fig. 1 demonstrates this by comparing aging curves for films of equivalent thickness and different applied tensions with films of different thickness and the same tension. To within experimental error, the measured physical aging rates were found to fall into two groups with an average aging value of $(3.52 \pm 0.98) \times 10^{-4}$ at low stress values, $\sigma \lesssim 8$ MPa, and $(8.03 \pm 0.21) \times 10^{-4}$ at high stress values, $\sigma \gtrsim 9.5$ MPa. Fig. 2 graphs the measured physical aging rate β as a function of applied stress σ for the 1440 kg mol^{-1} M_w PS films. The data appear to transition from a low aging rate plateau at small stress values to a higher aging rate plateau at larger stress, with the transition occurring over a relatively small range of stress values around $\sigma \approx 8$ MPa. The higher aging rates at larger stress values indicate that the resulting polymer glass is less stable. Data for a second high molecular weight and monodisperse PS, 650 kg mol^{-1} M_w, are also included in Fig. 2 and fall within the range of data for the 1440 kg mol^{-1} M_w PS films.

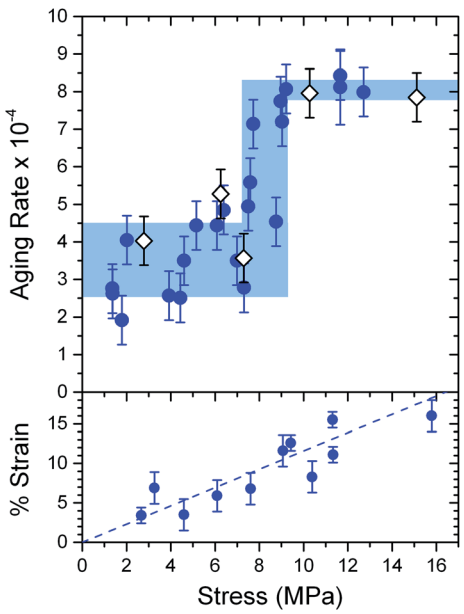

Fig. 2 Stress applied during vitrification increases subsequent physical aging rate of the glassy polymer film above a minimum stress value of $\sigma \approx 8$ MPa. Measured aging rate β as a function of stress applied for 2 min prior to and during thermal cooling for films of high molecular weight, monodisperse ($M_w/M_n = 1.04$–1.06) PS with $M_w = 1440$ kg mol^{-1} (solid blue circles) and $M_w = 650$ kg mol^{-1} (open black diamonds). The blue shaded bar is centered on the average value above and below the sharp transition in aging rate and represents the standard deviation of the measured data, while the vertical blue bar indicates the range of stresses over which the aging rate increases rapidly. (These bars are included only as a to guide the eye, and to enable easy comparison with the lower molecular weight data presented in Fig. 3b.) The error bars on each data point (±0.65) correspond to the standard deviation in aging rate of five different aging runs at a single stress value, while the applied stress is known to within 0.5 MPa, corresponding to the width of the symbols. The measured strain resulting from the applied stress is also plotted and is linear over the range of stresses investigated despite the large and sharp increase in aging rate.

The physical aging at non-zero stress is consistent with expectations for a non-equilibrium glass formed by a standard temperature quench. The plateau in aging rate at small stress values is consistent with recent work by Lee and Ediger[37] that found no change in aging rate for polymer glasses (formed stress free) subjected to small deformations. It is also perhaps intuitive that the aging rate should increase with applied stress. However, we find the qualitative behavior of the data most surprising, as it transitions quite sharply from a low stress aging response to higher aging rates at larger stress and appears to plateau. Whether this plateau would continue for even larger stress values is not clear because further measurements at larger stress are prevented by film failure. The variability in the data is slightly larger at the lower aging rates because the overall decrease in thickness with aging time is smaller. For an aging rate of 4×10^{-4}, the total decrease in film thickness during the 6 h of aging is only 0.04%, which for a 400 nm thick film corresponds to a decrease of 0.16 nm in thickness. Even though this decrease is very small, we have previously demonstrated[2,4,36] that it is within the sensitivity of our ellipsometer, and that this method of determining the physical aging rate from the decrease in film thickness is consistent with other methods using the increase in index of refraction, as well as other experimental techniques such as dilatometry.[36]

Fig. 2 also plots the measured strain achieved due to the applied stress on the polymer film in its rubbery state above T_g. The data show a linear trend over the range of applied stresses despite the sharp increase in aging rates observed indicating that the rubbery film behaves as expected for an elastic material, with no unusual change in deformation occurring at the stress where the increase in aging rate is observed. For an elastic rubber, the observed strains (all <20%) are sufficiently small that no appreciable chain alignment would be anticipated, consistent with our observation that no evidence of birefringence is measured (differences in index of refraction were <|0.003|) even for the largest strains. When stress was applied, the films immediately stretched to their total elongation and did not visibly lengthen with time during the short two minutes stress was applied prior to thermally quenching the films. Such an observation is consistent with a tensile creep compliance deformation into the entanglement plateau region where strain does not depend on time for times less than the reptation time. At a temperature of $T_g + 20$ °C, the reptation time is 24 min for 650 kg mol^{-1} M_w PS and 6 h for 1440 kg mol^{-1} M_w PS. Thus above T_g, our films are equivalent to a rubbery, physically cross-linked network. When samples are annealed for longer times comparable to the reptation time, flow occurs and the films lose mechanical integrity.

Interestingly, the effective compliance of the strain–stress data shown in Fig. 2, 1.2×10^{-8} Pa^{-1}, is smaller by two orders of magnitude than the anticipated bulk plateau compliance of PS, 4×10^{-6} Pa^{-1} (estimating a bulk uniaxial elongational compliance D from a plateau shear compliance[38] of $\log J_e = -5.9$ *via* $J = 3D$, valid in the elastic regime). This indicates an increased stiffness of our films in the rubbery regime above T_g, which appears to be independent of film thickness over the range (150–700 nm) studied. Such stiffening has been previously observed in biaxial compliance measurements on ultrathin PS "nanobubble" films[39–41] and in nanoprobe contact measurements on a variety of polymers.[42–44] Despite considerable efforts, the underlying cause of this stiffening in thin films has yet to be identified, with suggestions that the effect is related to a stress-induced stiffening[43,44] or some change (trapping) of entanglements resulting from confinement of the polymer chains that may suppress some Rouse modes.[45,46] Clearly, more work is needed to understand this effect.

In an effort to determine how universal this unusual aging behavior is, we collected similar data for a lower and more disperse molecular weight distribution PS, 289 kg mol^{-1} M_w with $M_w/M_n = 2.19$, which is more typical of commercial polymers. As shown in Fig. 3, the observed behavior in physical aging rate as a function of applied stress during glass formation is qualitatively the same. The average aging rate for low stress values, $(3.53 \pm 0.61) \times 10^{-4}$, is the same as that for the higher molecular weight samples shown in Fig. 2, with the data tending to the same aging rate in the limit of zero stress. This is consistent with physical aging measurements of polymer glasses formed at nominally zero stress that do not show a molecular weight dependence as structural relaxation involves motion on a local segmental scale. The aging rate at zero stress is also in good agreement with recent work in our group on PS films subjected to biaxial stress on cooling imparted by thermal expansion mismatch between the film and supporting frame giving a limiting zero stress aging rate of $\sim 4 \times 10^{-4}$.[5]

Despite the qualitative similarities between the data in Fig. 3b and 2, there are some important differences. The transition from a low to high aging rate plateau with increasing stress appears sharper and more distinct. In addition, the resulting higher aging rate plateau is slightly reduced with an average aging rate of $(6.72 \pm 0.39) \times 10^{-4}$. (Stresses above 7.2 MPa could not be applied to this polymer as mechanical failure of the samples occurred.) Most significantly, the minimum stress needed before an increase in aging rate is observed is noticeably lower at $\sigma \approx 3$ MPa. These differences may be due to either the reduced molecular weight or the increased dispersity of the 289 kg mol^{-1} M_w PS. The reptation time for this polymer is only 90 s at the temperature (T_g + 20 °C) at which the two minutes of stress is applied; thus, partial relaxation of the material could occur for these samples. To test this assertion, several attempts were made to study a low molecular weight monodisperse PS (M_w = 400 kg mol^{-1}, M_w/M_n = 1.06), which were annealed and stressed for times (2–5 min) approaching and comparable to the reptation time (4.6 min). In all instances, these samples lost mechanical integrity during the stressing above T_g, which is consistent with our assertion and would be expected for polymer melts under stress in the flow regime. Thus, it is likely that the broad dispersity of the low molecular weight 289 kg mol^{-1} M_w PS samples, whose distribution contains some high molecular weight chains, allows for the samples to maintain mechanical integrity for the two minutes stress is applied above T_g. A significant presence of lower molecular-weight component within this distribution may then limit local stretching for a fraction of the chains. A full study of how the minimum stress and high aging rate plateau vary with molecular weight, dispersity, and annealing time is beyond the scope of the present work. Future studies could test these different factors by using various bimodal distributions of two monodisperse polymers to control the contributions of low and high molecular weight chains. These issues highlight the challenges of such measurements where stress is applied in the liquid state prior to vitrification. Such considerations would also make these types of studies difficult on other (unentangled) glassy systems, although one could imagine designing some experimental setup to apply compressive stresses that would presumably avoid this issue.

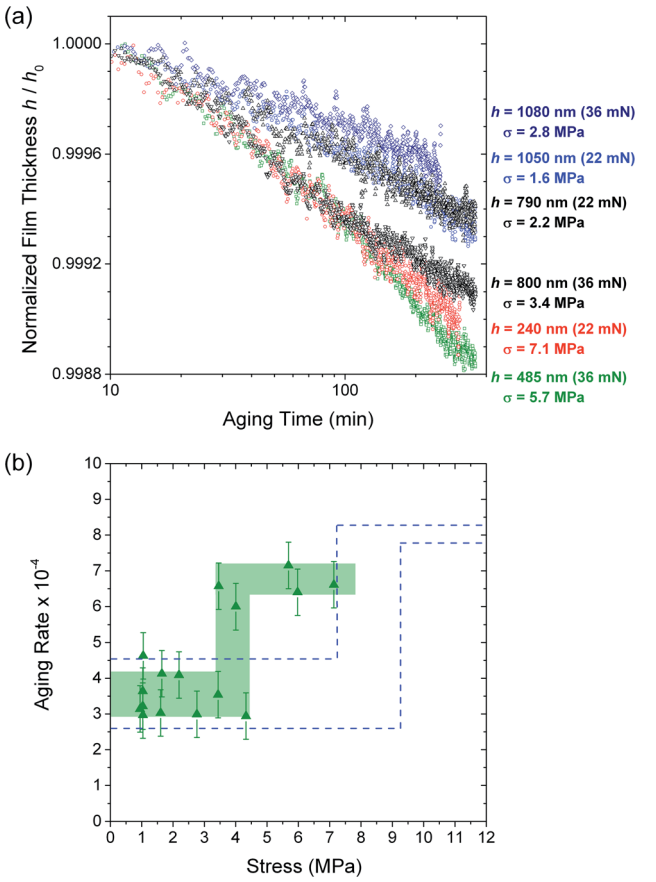

Fig. 3 Comparison of lower molecular weight polymer with broader dispersity. (a) Normalized film thickness h/h_0 *versus* logarithm of aging time for polydisperse PS with $M_w = 289$ kg mol^{-1} and $M_w/M_n = 2.19$. (b) Resulting physical aging rate β for films quenched under an applied stress σ during vitrification demonstrating an increased aging rate above a minimum stress. The shaded green bar highlights the average and standard deviation of the data, while the dashed blue lines indicate the range of high molecular weight data from Fig. 2.

We now consider possible reasons for the surprising qualitative shape of the aging rate β *versus* applied stress σ data presented in Fig. 2 and 3b. As the applied stress increases, the physical aging rate remains unchanged at low stresses, then above some minimum stress value, the aging rate transitions quickly over a small range of stresses to a higher aging rate before appearing to reach some new plateau. Although much work has investigated how the presence of stress can lead to enhanced mobility in glasses, the vast majority of the available literature on this pertains to glassy systems that were first formed stress free. Here, our experiments investigate for the first time the subsequent stability of glasses which have been formed by a temperature quench at non-zero stress values, as illustrated in Fig. 4a.

Our observation that the aging rate increases with applied stress demonstrates that the resulting glassy state is less stable. Consider a glass formed by cooling quickly, which exhibits a faster aging rate, indicative that it fell out of equilibrium at a higher temperature and formed a less stable glass. Within the PEL framework, the faster aging rates of quickly cooled glasses are seen to represent the more shallow energy basins higher in the PEL,[18,21] while glasses cooled more slowly are able to reach deeper energy metabasins lower in the PEL (Fig. 4b). Thus, from the faster aging rates observed at higher stress values, we can infer that the glassy state formed under large applied stress resides in a higher, less stable part of the PEL. The current theoretical understanding of how stress alters the mobility of glasses is also based on the glass' position within the PEL,[16,17] and not, as one might intuitively guess, on the available free volume because even glasses under compressive deformation show enhanced mobility.[14,15]

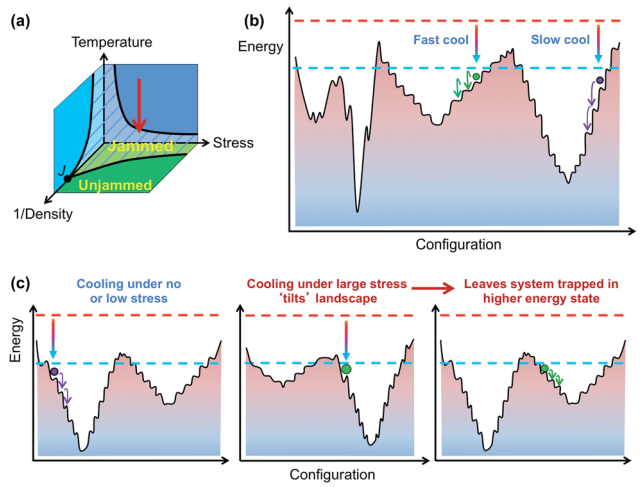

Fig. 4 Conceptual representation illustrating how stress during vitrification could alter stability of subsequent glassy material. (a) Jamming phase diagram indicating possible equivalence of temperature, density, and applied stress. Downward arrow emphasizes we are entering the jammed or glassy region of the phase diagram at a non-zero stress value. (b) Schematic potential energy landscape (PEL) of a typical glass former. As temperature is lowered, the system is trapped in a local 'metabasin' whose energy depends on cooling rate. Faster cooling rates trap the system into shallower, higher energy metabasins with correspondingly faster physical aging rates. (c) Proposed effect of stress during glass formation on local PEL. For large enough stress values, the PEL is sufficiently 'tilted' that on cooling the system ends up trapped in a different, higher energy metabasin, exhibiting a correspondingly faster physical aging rate even after the stress is removed.

To understand how stress might affect glass formation during a temperature quench, we propose an interpretation of our results based on the available literature investigating the deformation of glasses that have been formed stress free. We suggest that stress imparted to the material during glass formation acts to distort the PEL such that for high enough stress values above some minimum threshold value, the system preferentially cools into a different metabasin upon vitrification. After the stress is removed, the system is left trapped in this different, higher energy metabasin with a correspondingly faster physical aging rate (Fig. 4c). This interpretation is supported by observations that mobility of glasses depends on its position within the PEL,[16,17] and that stress or strain imparted to glasses and jammed systems lead to increased mobility.[11–13,23,24,28–31] These observations have been interpreted as a tilting of the PEL[17,22–27,29,37] acting to drive the system up the landscape,[23] which for sufficient magnitude can leave the system trapped in a higher energy state.[17,23] For example, in the work by Lee and Ediger,[37] small deformations of polymer glasses leave the physical aging rate unchanged indicating that the glass remains trapped within the same metabasin, while larger postyield deformations that can induce transitions to higher metabasins did appear to "rejuvenate" the glass as if it was thermally reset. This distinction between small and large deformations leading to qualitatively different aging behavior has been made by Lacks and Osborne[23] in their molecular dynamics simulations of sheared glasses where they find the system either "overaging" or "rejuvenating" depending on the size of the imposed strain. Within the PEL framework, small strains are seen as "overaging" the system, driving it towards the same, thermally defined energy minimum, whereas larger strains appear to "rejuvenate" the system by transitioning it to a shallower, strain-dependent energy minimum. The imposed deformation is treated as decreasing energy barriers between metabasins, which, if large enough, can facilitate the transition to a higher energy metabasin.[17,23,27]

In recent molecular dynamics simulations on a coarse-grained model of glassy PS, Chung and Lacks mapped the inherent structures of the system within the PEL for a PS glass subjected to shear strains.[27] For small strains, deformation was found to slowly drive the system up the landscape but remain within the same metabasin, while for larger strains, transitions to different, higher energy metabasins were observed. Similar results are found when stresses are applied.[26] Such simulations are consistent with our interpretation of the experimental results presented here. Our samples subjected to small deformations where the system quenches into the same metabasin would exhibit the same aging rate, while samples subjected to sufficiently large deformations that are enough to force the system to quench into a different, higher energy metabasin would lead to a higher aging rate. Although our data appear to show only a single transition to a higher energy metabasin, this does not preclude further transitions at higher stress, which

could not be reached in the present study because of film failure during stretching. Thus, in analogy to these works and other studies that treat mechanical deformation as facilitating energy barrier hopping by effectively 'tilting' the PEL,[17,23–27,29,37] we view the addition of stress during vitrification as altering the PEL landscape such that for sufficiently large stress the system can be left trapped in a different metabasin with a higher aging rate. This conceptual interpretation leaves many questions unanswered; however, we believe it provides a useful starting point for further investigations. Existing theories on glass deformation[17,23–25,27] and simulations that map the inherent structure of the PEL[16,27] could be adapted to verify this interpretation.

Our results demonstrate that the formation of a glass by a temperature quench under applied stress can lead to less stable glasses with faster physical aging rates above a minimum threshold stress. We interpret these results within the PEL framework as the applied stress acting to distort or tilt the landscape, which for sufficiently large values can leave the system trapped in a shallower, higher energy metabasin resulting in a less stable glassy state with faster structural relaxation. Vitrifying glasses under stress provides a means of accessing different parts of the PEL not necessarily accessible during thermal quenching, a process which could be used to manipulate the PEL and create glasses with different properties. Similarly, recent studies have found that manipulating the parameters of glass formation using controlled deposition conditions can produce glasses with unique material properties.[47–49] Understanding issues of how stress during glass formation alters the material's stability are particularly important for industrial applications involving polymers where various processing methods impart unintended stresses to the material, for example through thermal expansion mismatch between the polymer and mold.

The authors gratefully acknowledge support from Emory University and the Petroleum Research Fund (PRF-48927-DNI7).

Notes and references

1 R. D. Priestley, *Soft Matter*, 2009, **5**, 919–926.
2 J. E. Pye, K. A. Rohald, E. A. Baker and C. B. Roth, *Macromolecules*, 2010, **43**, 8296–8303.
3 J. E. Pye and C. B. Roth, *Phys. Rev. Lett.*, 2011, **107**, 235701.
4 L. A. G. Gray, S. W. Yoon, W. A. Pahner, J. E. Davidheiser and C. B. Roth, *Macromolecules*, 2012, **45**, 1701–1709.
5 J. E. Pye and C. B. Roth, *Macromolecules*, 2013, **46**, 9455–9463.
6 A. J. Liu and S. R. Nagel, *Nature*, 1998, **396**, 21–22.
7 A. J. Liu and S. R. Nagel, *Annu. Rev. Condens. Matter Phys.*, 2010, **1**, 347–369.
8 M. Pica Ciamarra, M. Nicodemi and A. Coniglio, *Soft Matter*, 2010, **6**, 2871–2874.
9 A. Ikeda, L. Berthier and P. Sollich, *Phys. Rev. Lett.*, 2012, **109**, 018301.
10 A. Ikeda, L. Berthier and P. Sollich, *Soft Matter*, 2013, **9**, 7669–7683.
11 V. Viasnoff and F. Lequeux, *Phys. Rev. Lett.*, 2002, **89**, 065701.
12 C. B. Roth, *J. Polym. Sci., Part B: Polym. Phys.*, 2010, **48**, 2558–2560.
13 G. B. McKenna, *J. Phys.: Condens. Matter*, 2003, **15**, S737–S763.
14 R. A. Riggleman, H.-N. Lee, M. D. Ediger and J. J. de Pablo, *Phys. Rev. Lett.*, 2007, **99**, 215501.
15 D. M. Colucci, P. A. O'Connell and G. B. McKenna, *Polym. Eng. Sci.*, 1997, **37**, 1469–1474.
16 R. A. Riggleman, K. S. Schweizer and J. J. de Pablo, *Macromolecules*, 2008, **41**, 4969–4977.
17 Y. G. Chung and D. J. Lacks, *J. Phys. Chem. B*, 2012, **116**, 14201–14205.
18 P. G. Debenedetti and F. H. Stillinger, *Nature*, 2001, **410**, 259–267.
19 F. H. Stillinger, *Science*, 1995, **267**, 1935–1939.
20 A. Heuer, *J. Phys.: Condens. Matter*, 2008, **20**, 373101.
21 S. Sastry, P. G. Debenedetti and F. H. Stillinger, *Nature*, 1998, **393**, 554–557.
22 H. Eyring, *J. Chem. Phys.*, 1936, **4**, 283–291.
23 D. J. Lacks and M. J. Osborne, *Phys. Rev. Lett.*, 2004, **93**, 255501.
24 K. Chen and K. S. Schweizer, *Europhys. Lett.*, 2007, **79**, 26006.
25 K. Chen and K. S. Schweizer, *Macromolecules*, 2011, **44**, 3988–4000.
26 C. E. Maloney and D. J. Lacks, *Phys. Rev. E: Stat., Nonlinear, Soft Matter Phys.*, 2006, **73**, 061106.
27 Y. G. Chung and D. J. Lacks, *Macromolecules*, 2012, **45**, 4416–4421.
28 L. S. Loo, R. E. Cohen and K. K. Gleason, *Science*, 2000, **288**, 116–119.
29 H. N. Lee, K. Paeng, S. F. Swallen and M. D. Ediger, *Science*, 2009, **323**, 231–234.
30 R. A. Riggleman, H.-N. Lee, M. D. Ediger and J. J. de Pablo, *Soft Matter*, 2010, **6**, 287–291.
31 E. I. Corwin, H. M. Jaeger and S. R. Nagel, *Nature*, 2005, **435**, 1075–1078.
32 L. C. E. Struik, *Physical Aging in Amorphous Polymers and Other Materials*, Elsevier Scientific Publishing Company, Amsterdam, 1978.
33 J. M. Hutchinson, *Prog. Polym. Sci.*, 1995, **20**, 703–760.
34 Y. P. Koh and S. L. Simon, *Macromolecules*, 2013, **46**, 5815–5821.
35 J. Zhao, S. L. Simon and G. B. McKenna, *Nat. Commun.*, 2013, **4**, 1783.
36 E. A. Baker, P. Rittigstein, J. M. Torkelson and C. B. Roth, *J. Polym. Sci., Part B: Polym. Phys.*, 2009, **47**, 2509–2519.
37 H. N. Lee and M. D. Ediger, *Macromolecules*, 2010, **43**, 5863–5873.
38 D. J. Plazek and V. M. O'Rourke, *J. Polym. Sci., Part A-2*, 1971, **9**, 209–243.
39 P. A. O'Connell and G. B. McKenna, *Science*, 2005, **307**, 1760–1763.
40 P. A. O'Connell and G. B. McKenna, *Eur. Phys. J. E*, 2006, **20**, 143–150.
41 P. A. O'Connell and G. B. McKenna, *J. Polym. Sci., Part B: Polym. Phys.*, 2009, **47**, 2441–2448.
42 H. D. Rowland, W. P. King, J. B. Pethica and G. L. W. Cross, *Science*, 2008, **322**, 720–724.

43 C. A. Tweedie, G. Constantinides, K. E. Lehman, D. J. Brill, G. S. Blackman and K. J. Van Vliet, *Adv. Mater.*, 2007, **19**, 2540–2546.
44 W. Xu, N. Chahine and T. Sulchek, *Langmuir*, 2011, **27**, 8470–8477.
45 P. A. O'Connell, S. A. Hutcheson and G. B. McKenna, *J. Polym. Sci., Part B: Polym. Phys.*, 2008, **46**, 1952–1965.
46 K. L. Ngai, D. Prevosto and L. Grassia, *J. Polym. Sci., Part B: Polym. Phys.*, 2013, **51**, 214–224.
47 S. F. Swallen, K. L. Kearns, M. K. Mapes, Y. S. Kim, R. J. McMahon, M. D. Ediger, T. Wu, L. Yu and S. Satija, *Science*, 2007, **315**, 353–356.
48 S. Singh, M. D. Ediger and J. J. de Pablo, *Nat. Mater.*, 2013, **12**, 139–144.
49 Y. Guo, A. Morozov, D. Schneider, J. W. Chung, C. Zhang, M. Waldmann, N. Yao, G. Fytas, C. B. Arnold and R. D. Priestley, *Nat. Mater.*, 2012, **11**, 337–343.